The Journal of Experimental Biology 201, 2171–2181 (1998)
Printed in Great Britain © The Company of Biologists Limited 1998
JEB1472

BURROW VENTILATION IN THE TUBE-DWELLING SHRIMP *CALLIANASSA SUBTERRANEA* (DECAPODA: THALASSINIDEA)

III. HYDRODYNAMIC MODELLING AND THE ENERGETICS OF PLEOPOD PUMPING

EIZE J. STAMHUIS* AND JOHN J. VIDELER
Department of Marine Biology, University of Groningen, PO Box 14, 9750 AA Haren, the Netherlands
*e-mail: e.j.stamhuis@biol.rug.nl

Accepted 5 May; published on WWW 25 June 1998

Summary

The process of flow generation with metachronally beating pleopods in a tubiform burrow was studied by designing a hydrodynamic model based on a thrust–drag force balance. The drag of the tube (including the shrimp) comprises components for accelerating the water into the tube entrance, for adjusting a parabolic velocity profile, for accelerating the flow into a constriction due to the shrimp's body and another constriction due to the extended tail-fan, for shear due to separation and for the viscous resistance of all tube parts. The thrust produced by the beating pleopods comprises components for the drag-based thrust and for the added-mass-based thrust. The beating pleopods are approximated by oscillating flat plates with a different area and camber during the power stroke and the recovery stroke and with a phase shift between adjacent pleopod pairs. The added mass is shed during the second half of the power stroke and is minimized during the recovery stroke. A force balance between the pleopod thrust and the tube drag is effected by calculating the mean thrust during one beat cycle at a certain flow velocity in the tube and comparing it with the drag of the tube at that flow velocity. The energetics of the tube and the pump are derived from the forces, and the mechanical efficiency of the system is the ratio of these two. Adjusted to standard *Callianassa subterranea* values, the model predicts a mean flow velocity in the tube of 1.8 mm s^{-1}. The mean thrust force, equalling the drag, is 36.8 μN, the work done by the pleopod pump per beat cycle is 0.91 μJ and the energy dissipated by the tube system is 0.066 μJ per cycle. The mechanical efficiency is therefore 7.3 %. Pump characteristics that may be varied by the shrimp are the beat frequency, the phase shift, the amplitude and the difference in pleopod area between the power and recovery strokes. These parameters are varied in the model to evaluate their effects. Furthermore, the moment of added mass shedding, the distance between adjacent pleopods, the number of pleopods and the total tube drag were also varied to evaluate their effects.

Key words: burrow ventilation, tube-dwelling shrimp, *Callianassa subterranea*, ventilation energetics, laminar flow, hydrodynamic modelling.

Introduction

Most tube-living crustaceans use the thrust generated by beating limbs to ventilate their burrow (Atkinson and Taylor, 1988; Allanson *et al.* 1992). The thalassinid decapods beat three or four pairs of pleopods metachronally (Farley and Case, 1968; Dworschak, 1981). Burrow ventilation is assumed to be energetically expensive and is always a periodic event (Atkinson and Taylor, 1988; Farley and Case, 1968; Torres *et al.* 1977; Felder, 1979; Dworschak, 1981; Mukai and Koike, 1984; Scott *et al.* 1988; Forster and Graf, 1995; Stamhuis *et al.* 1996). The ventilation flow rates of the Callianassidae vary between 0.6 and 10 ml min^{-1} (Koike and Mukai, 1983; Mukai and Koike, 1984; Forster and Graf, 1995; Stamhuis and Videler, 1997*b*), and those of the Upogebiae vary between 33 and 50 ml min^{-1} (Dworschak, 1981; Koike and Mukai, 1983). Descriptions of sediment resuspension in tropical Callianassidae and respiratory ventilation in Upogebiae suggest even higher ventilation capacities (e.g. de Vaugelas, 1985; Scott *et al.* 1988). The energy involved in burrow ventilation has been estimated from the ventilation flow rates in a few shrimp species only (Gust and Harrison, 1981; Allanson *et al.* 1992; Stamhuis and Videler, 1997*b*). These estimates of the dissipated energy are based on the resistance of the tube, without taking the mechanism of flow generation into account. They therefore underestimate the total energy invested by the pumping shrimp (Stamhuis and Videler, 1997*b*).

The thalassinid shrimp *Callianassa subterranea* creates and inhabits an extensive burrow in the seabed (Witbaard and Duineveld, 1989; Atkinson and Nash, 1990; Rowden and Jones, 1995; Stamhuis *et al.* 1997). The shrimp ventilates the burrow on average every 14 min for approximately 1.3 min, which represents 8 % of its time budget (Stamhuis *et al.* 1996).

The ventilation flow is produced by active pumping using three pairs of pleopods in an ad-locomotory metachronal pattern at a frequency of approximately 1 Hz. The pleopods are spread during the power stroke and retracted during the recovery stroke. The areas of the pleopods differ by a factor of approximately two between these strokes (Stamhuis and Videler, 1997*a*). Although the beat pattern is rhythmical, the flow generated in the burrow is non-pulsatile and completely laminar. In the vicinity of the beating pleopods, the main flow is confined to the lower part of the tube, owing to a constriction caused by the tail-fan (Stamhuis and Videler, 1997*b*). The kinematics of the structures involved in burrow ventilation and the resulting flow patterns in the vicinity of the shrimp are reasonably well understood, but the mechanisms of thrust production and the energy involved in ventilation need more investigation. The present study therefore concentrates on mapping the thrust and drag forces generated by *Callianassa subterranea* and on the energy involved in ventilation by applying hydrodynamic modelling. The dissipated mechanical energy of pumping is estimated by adapting a more generally applicable model to the pumping characteristics of the shrimp. The effects of varying characteristic variables on the flow velocity in the tube, the dissipated mechanical energy and the pump efficiency are evaluated.

Materials and methods

The tube-pump model

A shrimp ventilating its burrow is essentially a pump driving water through a tube. When the flow velocity is constant, the thrust-producing pump is counteracted by the resistance of the tube. The mean thrust will equal the mean drag, and the forces are in equilibrium:

$$\bar{F}_{\mathrm{thr,pump}} = -\bar{F}_{\mathrm{d,tube}}\,. \tag{1}$$

Both the thrust and the drag are a function of the flow velocity in the tube. To determine the magnitude of the thrust and the drag, equation 1 must be solved numerically with the flow speed in the tube as an iteration variable.

Tube drag

The drag of the tube, including the shrimp's body, is calculated by summing the drag contributions of the separate parts of the tube, applying the approach of Stamhuis and Videler (1997*b*). The flow in the tube is assumed to be laminar (Hagen–Poiseuille flow) with a mean flow velocity. The tube containing the animal is abstracted to be a straight cylindrical tube, of length L_{tot} and diameter D_1, with two constrictions (Fig. 1). The first constriction is a reduction of the tube cross-sectional area A to $A_2=C_{\mathrm{body}}A_1$, where C_{body} is the coefficient of tube area reduction due to the shrimp's body, over a distance L_2, representing the shrimp's body ($1>C_{\mathrm{body}}>0$, $A_1=\frac{1}{4}\pi D_1^2$). The second constriction, immediately behind the first, reduces the tube area to $A_{\mathrm{c}}=C_{\mathrm{c}}A_1$, where C_{c} is the coefficient of tube area reduction due to the tail-fan constriction. It represents the reduction in cross-sectional area by the uropods and the telson ($1>C_{\mathrm{c}}>0$). The cross-sectional area in the third part of the tube equals that in the first part ($A_3=A_1$).

The total drag force consists of the following components (Prandtl and Tietjens, 1957; Schlichting, 1979; Munson *et al.* 1994), where U is velocity, ρ is the density and μ is the dynamic viscocity of sea water: (a) the force related to accelerating water into the tube entrance = $\frac{1}{2}\rho U_1^2A_1$; (b) the drag associated with adjusting a parabolic velocity profile = $1.2\times\frac{1}{2}\rho U_1^2A_1$; (c) the viscous drag of the tube section upstream of the animal = $8\pi\mu L_1U_1$; (d) the force required to accelerate the flow into the first constriction = $\frac{1}{2}\rho\{U_1[(A_1/A_2)-1]\}^2A_2$; (e) the viscous drag of the first constricted section = $8\pi\mu L_2U_2$; (f) the force required to accelerate the flow into the second constriction = $\frac{1}{2}\rho\{U_2[(A_2/A_{\mathrm{c}})-1]\}^2A_{\mathrm{c}}$; (g) the drag involved in the flow separation directly behind the second constriction = $\frac{1}{2}\rho U_{\mathrm{c}}^2(1-A_{\mathrm{c}}/A_3)^2A_3$; and (h) the viscous drag of the tube section downstream of the animal = $8\pi\mu L_3U_3$.

The tube is divided into three sections with lengths L_1, L_2 and L_3 (see Fig. 1). The drag of the upstream section is the sum of the drag components a, b and c. Components d, e and f sum to form the drag of the middle section, and the sum of g and h represents the drag of the downstream section. The drag forces ($F_{1,\mathrm{d,tube}}$–$F_{3,\mathrm{d,tube}}$) of these sections can be written as specific equations by expressing all velocities U and tube diameters D as multiples or fractions of $\bar{U}$ and D_{tube}, where D_{tube} is the diameter of the tube:

$$F_{1,\mathrm{d,tube}} = \frac{2.2\rho\bar{U}^2\pi D_{\mathrm{tube}}^2}{8} + 8\pi\mu L_1\bar{U}\,, \tag{2}$$

$$F_{2,\mathrm{d,tube}} = \frac{\pi\rho\bar{U}^2D_{\mathrm{tube}}^2}{8}\left[\left(\frac{1}{C_{\mathrm{body}}}-1\right)^2 C_{\mathrm{body}} + \left(\frac{1}{C_{\mathrm{c}}}-\frac{1}{C_{\mathrm{body}}}\right)^2 C_{\mathrm{c}}\right] + 8\pi\mu L_2\,\frac{\bar{U}}{C_{\mathrm{body}}}\,, \tag{3}$$

$$F_{3,\mathrm{d,tube}} = \frac{\pi\rho\bar{U}^2D_{\mathrm{tube}}^2}{8}\left[\left(\frac{1}{C_{\mathrm{c}}}-1\right)^2(1-C_{\mathrm{c}})^2\right] + 8\pi\mu L_2\bar{U}\,. \tag{4}$$

The total tube drag is:

$$F_{\mathrm{d,tube}} = F_{1,\mathrm{d,tube}} + F_{2,\mathrm{d,tube}} + F_{3,\mathrm{d,tube}}\,. \tag{5}$$

The energy dissipated by the tube and the water flow during one beat cycle of the pleopods $W_{\mathrm{tube,T}}$ is the product of the drag force, the mean velocity and the duration of the beat cycle T:

$$W_{\mathrm{tube,T}} = F_{\mathrm{d,tube}}\times\bar{U}\times T\,. \tag{6}$$

Pleopod-generated thrust

The thrust generated by an oscillating pleopod pair is calculated by summing the drag forces and the forces required to accelerate the added mass of water around the pleopod. A pleopod pair is assumed to resemble a slightly cambered flat

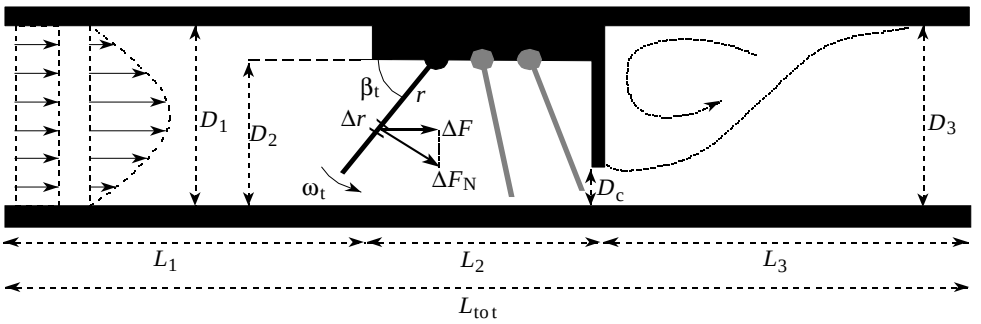

Fig. 1. Diagram of a model ventilating *Callianassa subterranea* in a tube, showing hydrodynamic events (dashed lines), cross-sectional ventilatory profiles (horizontal arrows) and variables used in the tube-pump model (see text). *D*, diameter; *L*, length; subscripts 1, 2, 3 and c refer to the respective tube sections and the narrow constriction; L_{tot}, total length of the tube; F_N, normal force; *r*, fraction of pleopod length; β_t, angle between tube axis and pleopod; ω_t, time-dependent angular velocity of a pleopod pair.

plate attached to the tube wall by a hinge. Each pair has its own sinusoidal motion pattern with time-dependent angular velocity ω_t. The relative velocity between a pleopod and the water depends on the phase of the oscillation as well as on the distance to the pleopod hinge. The force ΔF exerted on the water in the direction of the flow by a horizontal slice of a pleopod (height Δr and width w_{pp}) at distance *r* from the hinge (Fig. 1) can be expressed as the sum of a drag force F_d and an added mass force F_{am}:

$$\Delta F = \Delta F_d + \Delta F_{am} . \quad (7)$$

The drag force ΔF_d is derived from Newton's Resistance Law expressed as a Bernoulli-like dynamic pressure equation incorporating a drag coefficient C_d (Prandtl and Tietjens, 1957):

$$\Delta F_d = 0.5\rho C_d(w_{pp}\Delta r) \times |\omega r - U_y \sin\beta| \times (\omega r - U_y \sin\beta)\sin\beta , \quad (8)$$

where U_y is the velocity component perpendicular to the tube axis and β is the angle between the pleopod and the axis.

The drag coefficient C_d of a pleopod is assumed to equal the drag coefficient of a flat plate perpendicular to the flow $C_{d,fp}$, corrected for camber using a multiplication factor f_{cam}:

$$C_d = C_{d,fp} \times f_{cam} , \quad (9)$$

where $C_{d,fp}$ is a function of the Reynolds number *Re* based on the plate width (after Vogel, 1994):

$$C_{d,fp} = 1.17 + 17.1Re^{-1.21} \quad (10)$$

(N=7, $1<Re<10^6$, r^2=0.9996) and f_{cam} is a function of d/w_{pp}, where *d* is the camber depth and w_{pp} is the pleopod width, and of the direction of flow (Fig. 2, after Hoerner, 1965).

The added mass force ΔF_{am} is derived from Newton's Second Law of inertia and is essentially the product of the mass of a pleopod pair, including its water mantle, and the local acceleration. The mass of the flat-plate-like pleopods is assumed to be negligible compared with the added mass and is therefore omitted from the equation. The added mass of a pleopod section with a height Δr is assumed to equal the added mass of a section of an oscillating flat plate, being the mass of the volume of a cylinder with a diameter equal to the width w_{pp} and a height Δr (equalling the body of revolution around the longitudinal central axis) (Blake, 1979; Morris *et al.* 1985).

$$\Delta F_{am} = \rho(\tfrac{1}{4}\pi w_{pp}^2 \Delta r) \times \frac{d(\omega r)}{dt} \times \sin\beta , \quad (11)$$

where *t* is time.

The added mass forces are not constant throughout the beat cycle because they decrease with increasing Reynolds numbers (Vogel, 1994) and as a result of shedding of the water mantle (Daniel, 1984). Added-mass shedding at sinusoidally oscillating pleopods can be predicted from the limb kinematics and the resulting forces. The normal drag forces have been dealt with separately and are neglected here.

The added mass of a pleopod pair $M_{a,pp}$ is assumed to equal $\frac{1}{4}\rho\pi w_{pp}^2 R$, where *R* is pleopod length, with its centre of mass at $R/2$ (Fig. 3). At the start of a power stroke, the oscillating pleopod exerts a force $F_{am}=(d\omega/dt)\times M_{a,pp}\times(R/2)$ on the added mass, resulting in an acceleration $d(\omega R/2)/dt$ in the tangential direction. $M_{a,pp}$ is subjected to an additional radial (centrifugal) force

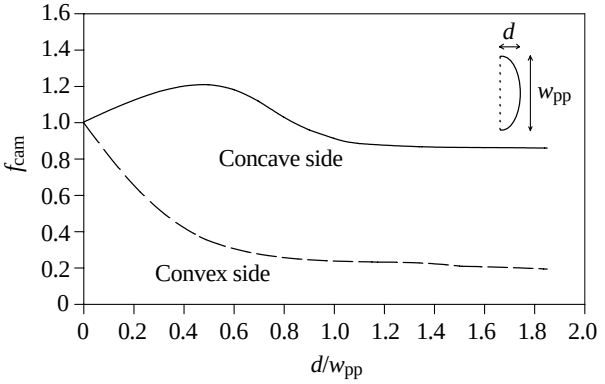

Fig. 2. The correction factor f_{cam} due to camber for the drag coefficient of a flat plate perpendicular to the flow, with flow towards the convex and towards the concave sides, as a function of d/w_{pp}, where *d* is camber depth and w_{pp} is plate width (based on data in Hoerner, 1965).

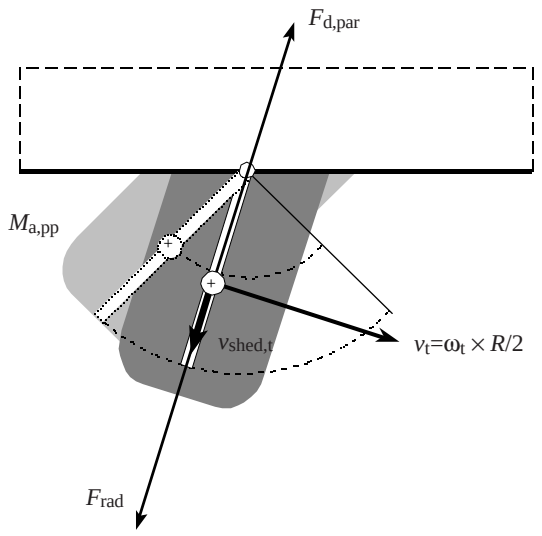

Fig. 3. Diagram depicting the radial forces on the added mass $M_{a,pp}$ of an oscillating pleopod, modelled as a flat plate. Velocity vectors in the radial and tangential directions are indicated. Vectors are not drawn to scale. The light shaded area indicates $M_{a,pp}$ at the start of the power stroke (t=0), the dark shading is for t≈0.15T after t=0, where t is time and T is the duration of the beat cycle. The centre of mass of $M_{a,pp}$ is depicted as a circle with a central plus sign. v_t, velocity of $M_{a,pp}$ in the tangential direction with respect to the pleopod; $v_{shed,t}$, radial velocity of $M_{a,pp}$ in the radial direction; F_{rad}, centrifugal force on the added mass of the pleopod in the radial direction; $F_{d,par}$, drag force parallel to the pleopod during added mass shedding; ω_t, time-dependent angular velocity of the pleopod pair; R, pleopod length.

$F_{rad}=M_{a,pp}\times v_t^2/(R/2)=M_{a,pp}\times\omega_t^2 R/2$, where v_t is the velocity of $M_{a,pp}$ in the tangential direction with respect to the pleopod. This force is the reactive force due to inertia because $M_{a,pp}$ resists changes in the direction of movement (Daniel, 1984). Thus, while $M_{a,pp}$ is accelerated in the tangential direction, it tends to move radially and is shed from the pleopod due to F_{rad}. However, as soon as $M_{a,pp}$ starts to move in the radial direction with respect to the pleopod, this motion is resisted by an induced drag force parallel to the pleopod: $F_{d,par}=\frac{1}{2}\rho C_{d,par} w_{pp} R v_{shed,t}^2$. $v_{shed,t}$ is the velocity of the added mass in radial direction, with $C_{d,par}$ being approximated by the drag coefficient of a flat plate parallel to the flow (after Vogel, 1994):

$$C_{d,par} = 0.004 + 12.4Re^{-0.91} \quad (12)$$

(N=7, 1<Re<10^6, r^2=0.99).

The Reynolds number of the pleopod is 100–200 half-way through the power stroke, resulting in a $C_{d,par}$ of 0.2–0.1. A dynamic equilibrium between F_{rad} and $F_{d,par}$ evolves. The radial velocity v_t increases during the first half of the power stroke, maintaining this force balance. F_{am} is zero half-way through the power stroke, but F_{rad} is maximal because ω_t is maximal. In the second half of the power stroke, the pleopod decelerates, but instead of decelerating with the pleopod, the added mass will continue moving caudally due to inertia and will slide off the pleopod in a radial direction. Note that there is no exact moment of shedding, but that the added mass sheds gradually. This process was simplified to implement it in our model by incorporating a coefficient C_{shed} setting the moment of instantaneous added mass shedding.

Because the water mantle is smaller during the recovery stroke than during the power stroke, the added-mass forces are assumed to be smaller during the recovery stroke than during the power stroke.

The thrust $F_{thr,t}$ produced by the whole pleopod pair at time t is found by integrating the thrust forces from the hinge to the tip of the pleopods:

$$F_{thr,t} = \int_0^R \mathrm{d}F \, . \quad (13)$$

The mean thrust $\bar{F}_{thr}$ during one motion cycle with period T is found by integrating $F_{thr,t}$ over a whole period divided by T:

$$\bar{F}_{thr} = \frac{1}{T}\int_0^T\int_0^R \mathrm{d}F\mathrm{d}t \, . \quad (14)$$

The rate of doing work per pleopod pair slice is the product of the velocity ($\omega r - U_y \sin\beta$) and the force dF. The total work per beat cycle per pleopod pair is then found by integrating over the pleopods from hinge to tip, and over time from 0 to T:

$$W_{thr,t} = \int_0^T\int_0^R (\omega r - U_y \sin\beta)\mathrm{d}F\mathrm{d}t \, . \quad (15)$$

The mechanical efficiency η of the pump-and-tube system described can be found by expressing the energy required to accelerate the water into the tube and to overcome the tube drag as a fraction of the total energy produced by the pump:

$$\eta = \frac{W_{tube,T}}{W_{thr,T}} \, . \quad (16)$$

A pump system consisting of more than one pleopod pair can be treated as an array of single pleopod pairs. However, phase shifts between adjacent pleopod pairs or very small distances between the pairs may result in direct interactions. These interactions will influence the net thrust forces and the energy produced as a result of masking effects. In this model, a pleopod pair is assumed not to contribute to drag or thrust as long as it is touching a more rostrally situated neighbouring pair.

Applying the tube-pump model to Callianassa subterranea

The morphology of the pleopods and the tail-fan, the approximation of the pleopod kinematics of *C. subterranea* and the flow in the vicinity of the shrimp, as described by Stamhuis and Videler (1997*a*,*b*), are used as input for the model.

During burrow ventilation of *C. subterranea*, the three pairs of sinusoidally beating pleopods are ranked from rostral to caudal and phase-shifted over 120°. As a result of the phase shift, the pleopods interact mainly during their recovery stroke. During these interactions, the caudal-most of two interacting pleopod pairs moves together with the rostral-most until it is able to resume its own sinusoidal path. Interactions are

assumed to take place when the pleopod tips overlap. During interactions, the caudal-most pleopod pair is assumed not to contribute to the thrust.

The camber of the pleopods is different during the two strokes. The camber depths are approximately $0.13w_{pp}$ during the power stroke and $0.30w_{pp}$ during the recovery stroke. The pleopod drag coefficients must therefore be multiplied by 1.08 during the power stroke and by 0.52 during the recovery stroke, indicating a slightly higher C_d during the power stroke and a significantly reduced C_d during the recovery stroke, compared with a flat plate.

In *C. subterranea*, the added mass of a pleopod is gradually shed in a caudo-ventral direction during the second half of the power stroke and is relatively small during the recovery stroke. In the model, instantaneous shedding half-way through the power stroke is assumed, and the added mass forces are therefore assumed to be zero during the second half of the power stroke. During the recovery stroke, the water mantle comprising the added mass is assumed to be reduced to 20 % of its initial volume.

At rest, a pleopod has an angle of $\beta_0=\pi/2$ with respect to the tube axis. The pleopods oscillate sinusoidally with a maximum angle swept α_0. The angular velocity of a pleopod at time t is:

$$\omega_t = \frac{d\beta_t}{dt} , \quad (17)$$

where β_t is the angle between the pleopod and the tube axis at time t:

$$\beta_t = \beta_0 + \alpha_0 \sin(\omega_t + \theta_n) , \quad (18)$$

and θ_n is the phase shift of the nth pleopod pair.

The flow in the burrow upstream and downstream of the shrimp is laminar with a parabolic velocity profile and is not pulsatile. At the abdomen of the shrimp, in the vicinity of the beating pleopods, the mean flow velocity $\bar{U}_y$ is assumed to increase linearly from 0 to $2\bar{U}$ downwards over the cross section of the tube (from dorsal to ventral with respect to the shrimp).

The mean flow velocity in the tube $\bar{U}$ is used as an iteration variable when implementing the model for *C. subterranea*. The mean thrust produced by the pleopods and the drag of the tube are calculated with $\bar{U}$ asymptotically approaching a value at which the drag equals the mean thrust within 10^{-9} N. This value represents approximately 0.01 % of the forces at equilibrium for 'standard' *C. subterranea* characteristics.

A 'standard' *C. subterranea* reduces the tube cross section to 70 % with its body and to 10 % with its tail-fan and has three pleopod pairs 10 mm wide and 8.5 mm long with a 120 ° phase shift and a 45 ° maximum angle swept. The area of the pleopods is assumed to be halved during the recovery stroke. The total tube length of the burrow is 0.45 m and the shrimp's body length is 0.05 m. The tube diameter is 0.01 m (Stamhuis and Videler, 1997*a*,*b*). The flow velocity, thrust and drag, as well as the energetics and the efficiency, are calculated at equilibrium of forces.

The beat frequency, phase shift, angle swept, pleopod area ratio, added mass shedding, inter-pleopod distance, number of pleopod pairs and burrow size are varied to study their effect on the flow velocity in the tube, on pumping energetics and on the efficiency of the pleopod pump system of *C. subterranea*.

Results

The tube-pump model with all variables set for a 'standard' *C. subterranea* in a 'standard' tube (see diagram in Fig. 1) predicts a mean flow velocity in the tube $\bar{U}$ of 0.0018 m s^{-1}. The mean thrust produced by the oscillating pleopods, balancing the total tube drag, is $\bar{F}_{thr}=F_{d,tube}=36.8\times10^{-6}$ N. The total work per beat cycle done by the pleopods is $W_{pp,T}=0.91\times10^{-6}$ J, and the total work dissipated by the tube and water per pleopod beat cycle is $W_{tube,T}=0.066\times10^{-6}$ J. The mechanical efficiency η is therefore 7.3 %.

The pleopod tip positions in time with respect to the telson are depicted in Fig. 4A, which shows two complete beat cycles. The first pleopod pair (PP1) is able to perform a complete sine wave, but the movements of the other two pairs (PP2 and PP3) are restricted by the first and the second pair respectively. Fig. 4B shows the thrust generated (F_{thr}) and its components as a function of time. Drag forces (F_d) are produced by all three pleopod pairs, although not in equal amounts. Added mass forces (F_{am}) are mainly generated by the first and the second pleopod pair and contribute significantly to the total thrust. Owing to the metachronal motion pattern, the third pleopod pair generates thrust only during the second half of its power stroke and, therefore, contributes mainly to the drag forces and little to the added mass forces. The net thrust forces only just become negative because there is always a pleopod pair performing a power stroke. The mechanical work done by the pleopods from the start of the cycle is depicted in Fig. 4C, which shows the cumulative work per beat cycle $W_{pp,T}$ for two complete cycles. Approximately 50 % of the work per beat cycle is done by the first pleopod pair; the third and second pair contribute approximately 15 % and 35 %, respectively.

Variables that may be altered by a pumping shrimp are the beat frequency f, the phase shift angle θ and the angle swept α. According to the model, the flow velocity $\bar{U}$ in the tube, the work W done by the pleopods and the mechanical efficiency all depend strongly on these variables.

The flow velocity increases almost linearly with an increase in frequency and the mechanical efficiency η asymptotically approaches 14 % at high frequencies. The mechanical work, however, increases with the square of the frequency, indicating that a frequency increase involves high additional costs (Fig. 5).

According to the model, the flow velocity $\bar{U}$ in the tube will be greatest if there is little or no phase shift θ (Fig. 6). When θ is small, all the pleopods are able to contribute to the thrust during their entire power stroke, without being restricted by adjacent pleopod pairs. The work per beat cycle $W_{pp,T}$ as well as η are also maximal at small θ and decrease with increasing θ due to interactions among the pleopod pairs. At values of θ above 180 °, a metachronal wave in the contra-locomotory

direction occurs, instead of the ad-locomotory wave normally applied by *C. subterranea* at θ=120°. The flow velocity is minimal at θ≈300°. At this point, the pleopods just mask one another in the contra-locomotory metachronal wave, which counteracts the difference in area during the power stroke and the recovery stroke. The small peak at θ≈150° is an effect of the interactions between the pleopods, as the pleopods just touch one another during a small part of the recovery stroke.

In the model, the thrust depends on the angle β between a pleopod and the tube axis (see Fig. 1). At very small maximum angles swept α, the thrust generated is relatively small, but almost all of it contributes to the net thrust, since β stays close to 90° during the whole cycle. At small values of α, the mechanical efficiency is therefore relatively high at almost 30%, as can be seen in Fig. 7. At higher values of α, the thrust generated is relatively large, but only part of this thrust contributes to the net thrust, and η decreases. The relationship between η and α depends not only on β, but also on the drag coefficient of the pleopods and on the interactions between adjacent pleopod pairs. The angular velocity ω is directly related to α since f is kept constant. The drag coefficient of the pleopods is approximately inversely related to ωr (see equation 10). Interactions between adjacent pleopod pairs start at values of α above 10°. The mean flow velocity $\bar{U}$ as well as η show changes in their slopes at α=10°, and other small but sudden changes at higher values of α are caused by changes in pleopod interactions (Fig. 7). Disregarding the pleopod interaction effects, η decreases approximately co-sinusoidally

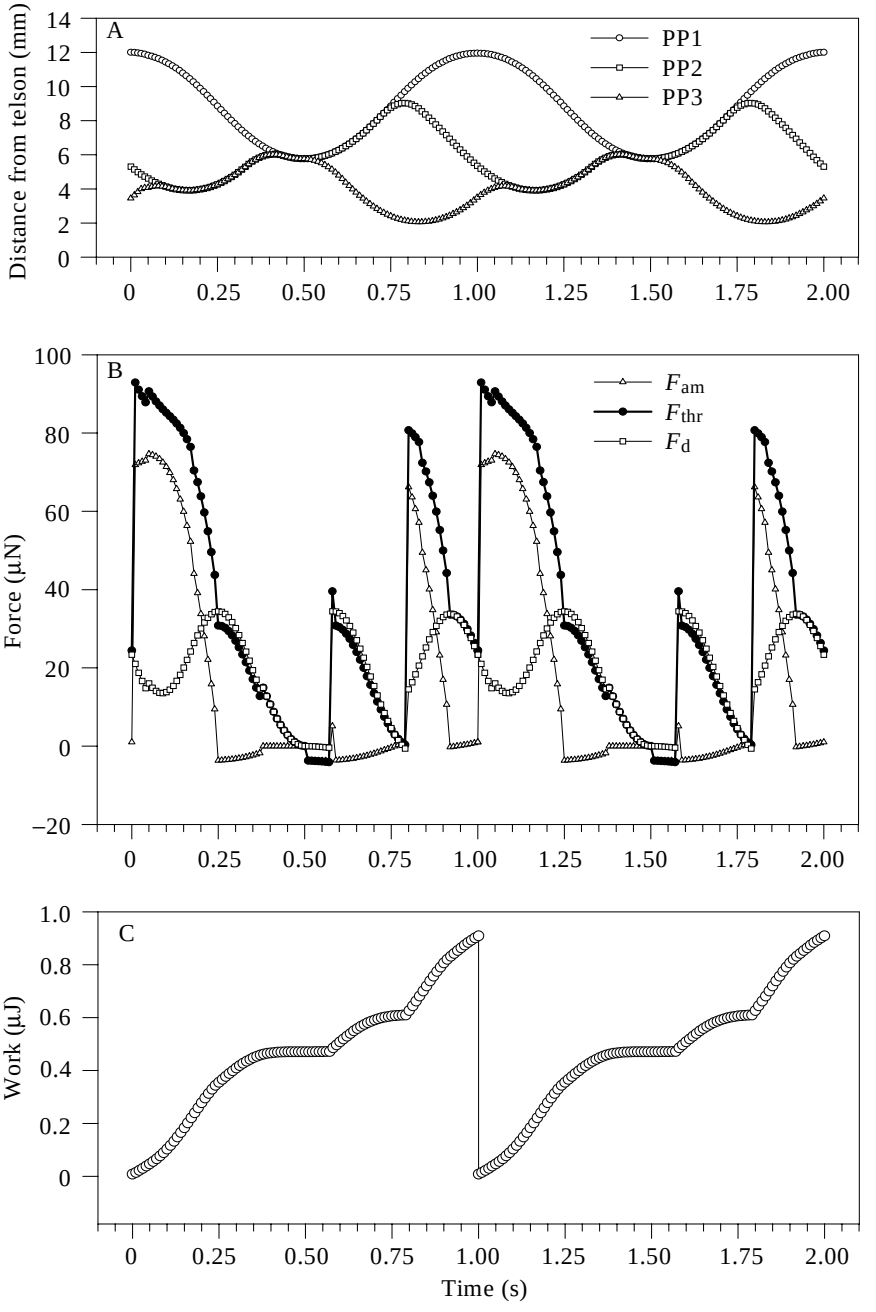

Fig. 4. The positions of the pleopod tips with respect to the telson (A), the generated thrust and its components (B) and the cumulative mechanical work (C) from the tube-pump model mimicking a ventilating *Callianassa subterranea*. To increase the clarity of the figure, one beat cycle is displayed twice. PP1–PP3, pleopods 1–3; F_{am}, added mass force; F_{thr}, thrust produced by one pleopod pair; F_d, drag force.

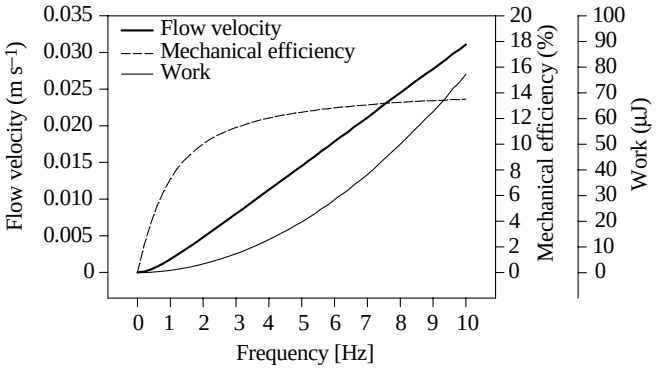

Fig. 5. The mean flow velocity in the tube $\bar{U}$, the mechanical efficiency η and the work done per beat cycle $W_{pp,T}$ as a function of the pleopod beat frequency f, predicted by the tube-pump model.

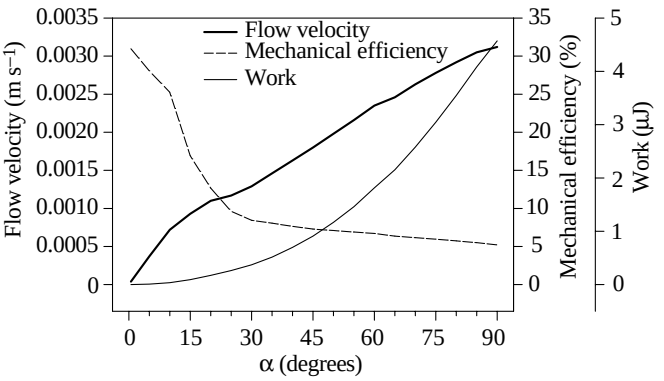

Fig. 7. The model predictions of the mean flow velocity in the tube $\bar{U}$, the mechanical efficiency η and the work done per beat cycle $W_{pp,T}$ as a function of the maximum pleopod angle swept α.

at small values of α due to decreasing β_{max}. At higher values of α, the η curve reflects the curve of the pleopod drag coefficient C_d as a function of Reynolds number due to the higher angular velocities. The work done by the pleopods per beat cycle $W_{pp,T}$ increases with the square of amplitude.

Fig. 8 shows that an increase in pleopod area during the recovery stroke $A_{pp,recovery}$ results in a gradual decrease in flow velocity in the tube. The value of η, however, decreases steeply at relatively larger pleopod areas during the recovery stroke, resulting in an increase in the work per beat cycle $W_{pp,T}$.

In the model, the added mass that is accelerated during the power stroke is assumed to be shed when the pleopod pair is half-way through the power stroke. This assumption is based on flow studies (Stamhuis and Videler, 1997*b*). Fig. 9 shows the effect of varying the moment of shedding during the power stroke expressed as a fraction of T in C_{shed}, on $\bar{U}$, η and $W_{pp,T}$. Shedding of the added mass at C_{shed}=0.25 (half-way through the power stroke) seems to yield the highest flow velocity in the tube and the highest mechanical efficiency. A delayed shedding, at C_{shed}≈0.35 results in a reduction in the work per cycle, because shedding takes place at the moment when the net thrust force approaches zero.

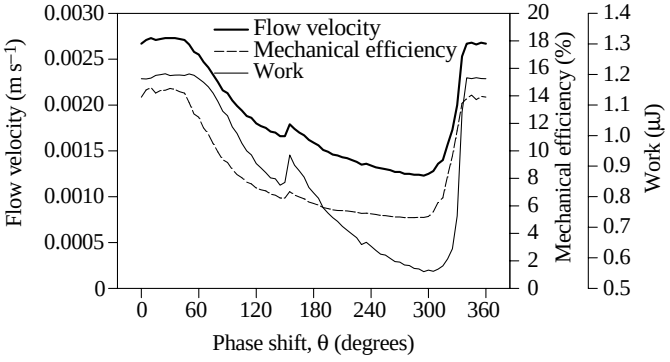

Fig. 6. The mean flow velocity in the tube $\bar{U}$, the mechanical efficiency η and the work done per beat cycle $W_{pp,T}$ as a function of the phase difference θ between adjacent pleopods, predicted by the tube-pump model.

The distance between adjacent pleopod pairs cannot be changed by a pumping *C. subterranea*, because it is completely determined by its morphology. In juveniles growing towards adulthood, however, the distances between the pleopod pairs increase with animal size. This may affect not only the absolute flow velocity in the tube but also the efficiency of the pump system and the work per beat cycle. Fig. 10 shows the effects of an increase in the distance between the adjacent pleopod pairs on $\bar{U}$, η and $W_{pp,T}$ as predicted by the model for a 'standard' *C. subterranea*. All three variables increase with increasing distance between the pleopod pairs, up to approximately 8 mm. Above 8 mm, all pleopod pairs are able to perform an almost complete power stroke and mask one another only during part of the recovery stroke. At distances greater than 11 mm, the pleopods no longer interact.

The number of pleopod pairs cannot be varied by *C. subterranea*. Some other thalassinid species, however, have four pairs of pleopods, and some tube-living invertebrates have many more paddling structures which are used for ventilation. The implications of more pairs of pleopods has

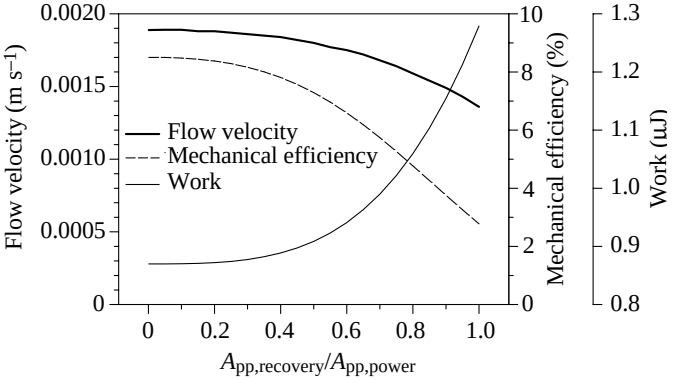

Fig. 8. The model predictions of the mean flow velocity in the tube $\bar{U}$, the mechanical efficiency η and the work done per beat cycle $W_{pp,T}$ as a function of the pleopod area ratio $A_{pp,recovery}/A_{pp,power}$, where power and recovery refer to the power and recovery strokes respectively.

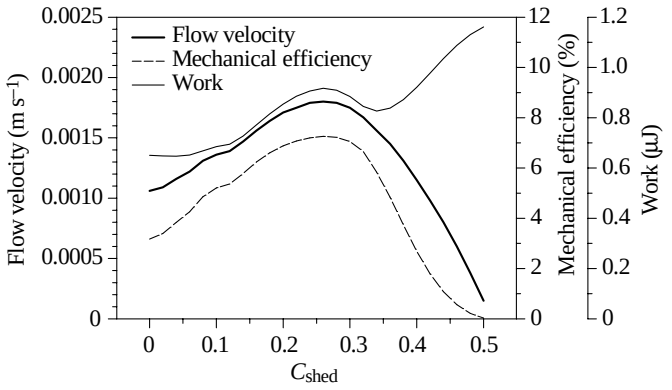

Fig. 9. The model predictions of the mean flow velocity in the tube $\bar{U}$, the mechanical efficiency η and the work done per beat cycle $W_{pp,T}$ as a function of the added mass shedding coefficient C_{shed}, which is expressed as a fraction of cycle duration.

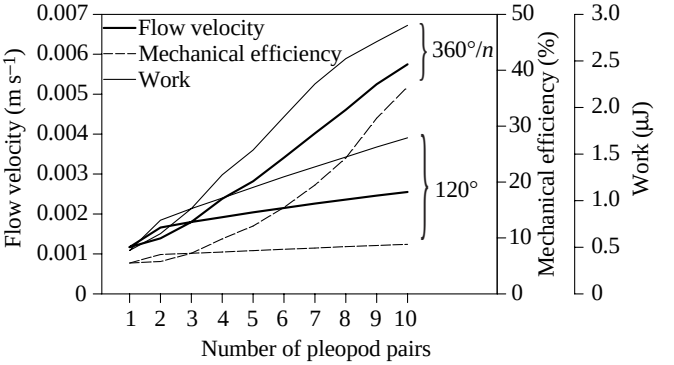

Fig. 11. The mean flow velocity in the tube $\bar{U}$, the mechanical efficiency η and the work done per beat cycle $W_{pp,T}$ as a function of the number of pleopod pairs n at a fixed phase shift θ=120 ° and at θ=360 °/n, predicted by the tube-pump model.

been evaluated by varying the number of pleopod pairs n from 1 to 10. Since in *C. subterranea* the phase shift between the pleopod pairs θ=360 °/n, the phase shift was set to vary along with n. For comparison, n was also varied without varying θ, but θ was kept at the 'standard' *C. subterranea* phase shift of 120 °.

With θ fixed at 120 °, the possession of more than one pleopod pair is clearly advantageous, but the flow velocity does not increase as much with n when there are more than two pairs (Fig. 11, lower set of curves). At n>2, the pump system does not change very much, and little additional thrust is added with every additional pair of pleopods, as reflected in the gradual rates of increase of $\bar{U}$, $W_{pp,T}$ and θ. When varying θ with n, the system changes with every additional pair of pleopods. The mechanical efficiency η increases more steeply than linearly with increasing n up to approximately eight pairs of pleopods (Fig. 11, upper set of curves). Above n=8, η still increases, although its slope as well as the slopes of $\bar{U}$ and $W_{pp,T}$ start to decrease. Note that at, for example, n=8 and θ=360 °/n=45 °, the flow velocity in the tube has doubled and the mechanical efficiency has quadrupled, at only double the cost compared with the situation with θ=120 °.

Burrow size is determined by the inhabiting *C. subterranea*. The effect of decreases as well as increases in burrow size are assumed to affect the burrow resistance. Changes in burrow resistance have been tested by multiplying the tube drag $F_{d,tube}$ by a factor b between 0 and 5 (Fig. 12). Since the flow velocity in the tube at standard settings (b=1) is only a fraction of the mean velocity of the pleopods, a decrease in burrow size results in an increase in the flow velocity in the tube. The total work done by the pleopods decreases and the mechanical efficiency increases dramatically with decreasing burrow size. An increase in burrow size does not result in dramatic changes, since all the variables shown are close to saturation. The flow velocity and the mechanical efficiency decrease slightly and the work done increases slightly. Apparently, the flow velocity in the burrow and the work done by the pleopods do not change very much above a critical burrow size, which is approximately 0.6 times the total tube length (L_{tot}) in our model.

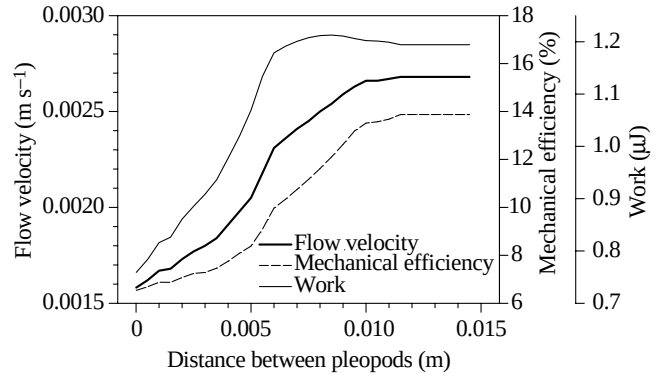

Fig. 10. The mean flow velocity in the tube $\bar{U}$, the mechanical efficiency η and the work done per beat cycle $W_{pp,T}$ as a function of the distance between adjacent pleopod pairs, predicted by the tube-pump model.

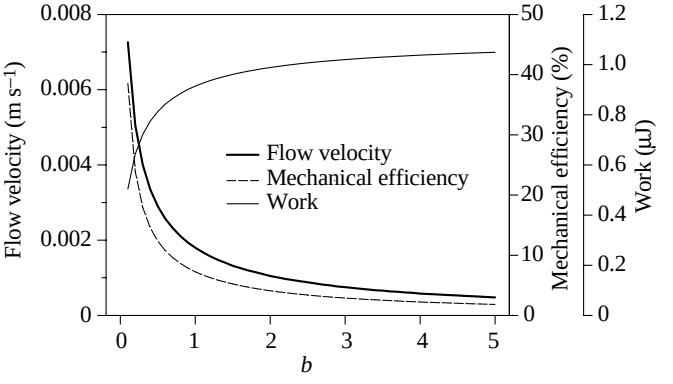

Fig. 12. The model predictions of the mean flow velocity in the tube $\bar{U}$, the mechanical efficiency η and the work done per beat cycle $W_{pp,T}$ as a function of the burrow size, expressed as b, where b is a constant varying from 0 to 5 by which $F_{d,tube}$, the drag force of the tube, is multiplied.

Discussion

Our tube-pump model predicts a mean flow velocity in the tube of 1.8 mm s^{-1} for a ventilating *C. subterranea* at 'standard' model settings. This is very close to the mean velocity of 2.0±0.1 mm s^{-1} actually generated by *C. subterranea* in an artificial burrow with characteristics similar to the model settings (Stamhuis and Videler, 1997*b*). Therefore, the model predictions for the mean thrust and drag forces, for the work done and for the mechanical efficiency are expected to be realistic.

The mean beat frequency during ventilation of *C. subterranea* is approximately 1 Hz. According to the model, the mechanical efficiency increases steeply in the frequency range 0–2 Hz and then levels off. The optimum beat frequency therefore seems to be approximately 2 Hz. However, the work per beat cycle increases with the square of frequency, so that doubling the frequency will quadruple the work per beat cycle. Sometimes the shrimp removes suspended sediment from its burrow by heavy ventilation movements lasting approximately 10 s at an estimated frequency of 3–5 Hz (Stamhuis *et al.* 1996). The work per beat cycle during such a pumping bout is up to 25 times the work during normal ventilation. Such an extreme effort will probably lead rapidly to energy depletion.

The phase shift between adjacent pleopod pairs in *C. subterranea* during normal ventilation is approximately one-third of the cycle. The model predicts the highest flow rates and mechanical efficiencies at small phase shift angles, at only a small increase of the work per cycle (25 %). It therefore seems optimal to apply an almost simultaneous beat pattern for all pleopod pairs. Such a pattern has been observed during propulsion of the copepods *Pleuromamma xiphias* and *Acanthocyclops robustus* (Morris *et al.* 1985, 1990). These species apply a small phase shift between the swimming legs during the power stroke only and perform a simultaneous recovery stroke. This results in maximum propulsive force for all swimming legs during the power stroke. The disadvantage of such a system, however, is that the thrust is generated in pulses, resulting in a jumpy swimming pattern. In *C. subterranea*, pulsatile thrust generation would probably lead to a pulsating flow in the tube, which is energetically disadvantageous (Stamhuis and Videler, 1997*b*). The hydrodynamic resistance of a tube increases dramatically with increasing pulsatility of the flow in the tube (Caro *et al.* 1978). A phase shift angle of 120 °, as found in *C. subterranea*, might therefore not be the theoretically optimal phase shift, but most probably helps to keep the flow in the tube steady and can be regarded as energetically advantageous.

A maximum angle swept of approximately 45 ° seems a good compromise between maximizing the flow velocity and minimizing the energetic costs. Differences in pleopod area between the power stroke and recovery stroke are determined mainly by the shrimp's morphology, and it is not surprising that a relatively smaller pleopod area during the recovery stroke should increase the flow velocity and the mechanical efficiency, at decreasing costs. It is, however, interesting to note that the actual ratio of the pleopod areas of *C. subterranea* of approximately 0.5 represents a critical value. The mechanical efficiency and the flow velocity start to decrease steeply around that value, and the work per beat cycle starts to increase drastically at this point (Fig. 8). A ratio closer to 1 would therefore be disadvantageous.

Shedding of added mass has not been incorporated quantitatively in previous models of paddling propulsion, although its importance has been pointed out (Daniel, 1984, 1995; Morris *et al.* 1990). Added mass shedding at the sinusoidally oscillating pleopods of *C. subterranea* can be predicted from their limb kinematics and the resulting forces on the added mass. We incorporated shedding of added mass as an instantaneous process in our model because this might mimic the real situation closely: the added mass is accelerated during the first half of the power stroke and subsequently shed with only very slight deceleration during the second half of that stroke (Stamhuis and Videler, 1997*b*). Variation of the moment of shedding in our model suggests that shedding the added mass at a C_{shed} ($=t_{shed}/T$, where t_{shed} is the time of added mass shedding) of 0.25–0.30, approximately half-way through the power stroke, is indeed most efficient.

In our calculations of the added mass component of the pleopod thrust, we assumed that the initial velocity of the added mass was zero. The velocity of the pleopod at that moment is zero ($\omega=0$) and, by definition, the added mass is the water mantle attached to the pleopod (Vogel, 1994). When the pleopod accelerates during the first part of the power stroke, the added mass must be accelerated as well. This process might be assisted by the flow in the lower part of the tube due to the high local flow velocities, but this contribution is hard to quantify. We did not take this into account and hence assume that the added mass forces are independent of the flow in the tube.

We varied the number of pleopods at different phase shifts in order to compare the thrust-producing system of *C. subterranea* with that of other tubiculous invertebrates and with that of free-swimming paddlers. With more than three pleopod pairs or other paddling structures, a phase shift smaller than 120 ° becomes advantageous. With more (pairs of) limbs, the mechanical efficiency of the propelling system increases significantly with the number of limbs at phase shifts of 360 °/n. This is observed, for example, in the brine shrimp *Artemia* swimming with up to 11 paddling thoracic appendages. The number of appendages depends on the developmental stage. The phase shift between pairs of trunk limbs is approximately one cycle divided by the number of active pairs, but minimally approximately one-ninth of a cycle (Barlow and Sleigh, 1980). Our model, although not originally developed for this type of free-swimming paddler, predicts an increase in the mechanical efficiency of trunk–limb propulsion with an increase in the number of trunk limbs during development towards adulthood. The model may, with a few modifications, be applicable to many other paddling animals, tubiculous or free-swimming.

List of symbols

A	cross-sectional area of tube section (m^2)
A_{pp}	area of pleopod pair (m^2)
b	constant with a value of 1–5
C_{body}	coefficient of tube area reduction due to the shrimp's body
C_c	coefficient of tube area reduction due to the tail-fan constriction
C_d	drag coeffient
$C_{d,fp}$	drag coefficient of a flat plate perpendicular to the flow
$C_{d,par}$	drag coefficient with the object parallel to the flow
C_{shed}	added mass shedding coefficient
d	pleopod camber depth (m)
D	diameter
D_{tube}	diameter of tube section (m)
f	frequency (Hz)
f_{cam}	C_d multiplication factor correcting for camber
F	force (N)
F_{am}	added mass force (N)
F_d	drag force (N)
$F_{d,par}$	drag force parallel to pleopod during added mass shedding (N)
$F_{d,tube}$	drag force of the tube (N)
F_N	normal force, perpendicular to the pleopod (N)
F_{rad}	centrifugal force on the added mass of the pleopod, in the radial direction (N)
F_{thr}	thrust force produced by beating pleopods (N)
$F_{thr,pump}$	thrust force produced by the pump (N)
$F_{thr,t}$	thrust force produced by a pleopod pair at time t (N)
L	length of tube section (m)
L_{tot}	total length of tube (m)
$M_{a,pp}$	added mass of pleopod (kg)
n	number of pleopod pairs
P	power ($J\,s^{-1}$)
r	fraction of pleopod length R (m)
R	pleopod length (m)
Re	Reynolds number
t	time (s)
t_{shed}	time of added mass shedding (s)
T	duration of the beat cycle, period (s)
U	velocity ($m\,s^{-1}$)
U_y	velocity perpendicular to the tube axis ($m\,s^{-1}$)
$v_{shed,t}$	velocity of $M_{a,pp}$ in radial direction with respect to the pleopod ($m\,s^{-1}$)
v_t	velocity of $M_{a,pp}$ in the tangential direction with respect to the pleopod ($m\,s^{-1}$)
w_{pp}	pleopod width (m)
W	work (J)
$W_{pp,T}$	work done per beat cycle (J)
$W_{thr,t}$	work done by a pleopod pair at time t (J)
$W_{tube,T}$	total energy dissipated by the tube and water flow during one beat cycle (J)
α	angle swept by a pleopod (degrees)
α_0	maximum angle swept by a pleopod (degrees)
β	angle between pleopod and tube axis (degrees)
β_{max}	maximum angle between pleopod and tube axis (degrees)
β_t	angle between pleopod and tube axis at time t (degrees)
β_0	angle between pleopod and tube axis at rest (degrees)
η	mechanical efficiency
μ	dynamic viscosity ($kg\,m^{-1}\,s^{-1}$)
ρ	density ($kg\,m^{-3}$)
θ	phase shift angle (degrees)
θ_n	phase shift of the nth pair of pleopods
ω	angular velocity ($rad\,s^{-1}$)
ω_t	time-dependent angular velocity

Subscripts

1, 2, 3	tube sections 1, 2 and 3, respectively
c	narrow constriction of the tube
recovery	recovery stroke
power	power stroke

We cordially thank Professor T. J. Pedley (University of Cambridge) for guidance on the fluid dynamics of tube flows, especially on entrance effects and oscillatory flow.

References

ALLANSON, B. R., SKINNER, D. AND IMBERGER, J. (1992). Flow in prawn burrows. *Est. Coast. Shelf Sci.* **35**, 253–266.

ATKINSON, R. J. A. AND NASH, R. D. M. (1990). Some preliminary observations on the burrows of *Callianassa subterranea* (Montagu) (Decapoda: Thalassinidea) from the west coast of Scotland. *J. nat. Hist.* **24**, 403–413.

ATKINSON, R. J. A. AND TAYLOR, A. C. (1988). Physiological ecology of burrowing decapods. In *Aspects of Decapod Crustacean Biology* (ed. A. A. Fincham and P. S. Rainbow). *Symp. zool. Soc. Lond.* **59**, 201–226. Oxford: Clarendon Press.

BARLOW, D. L. AND SLEIGH, M. A. (1980). The propulsion and use of water currents for swimming and feeding in larval and adult *Artemia*. In *The Brine Shrimp*, vol. 1 (ed. G. Persoone, P. Sorgeloos, O. Roels and E. Jaspers), pp. 61–73. Wetteren, Belgium: Universal Press.

BLAKE, R. W. (1979). The mechanics of labriform locomotion. I. Labriform locomotion in the angelfish (*Pterophyllum eimekei*), an analysis of the power stroke. *J. exp. Biol.* **82**, 255–271.

CARO, C. G., PEDLEY, T. J., SCHROTER, R. C. AND SEED, W. A. (1978). *The Mechanics of the Circulation*. Oxford: Oxford University Press.

DANIEL, T. L. (1984). Unsteady aspects of aquatic locomotion. *Am. Zool.* **24**, 121–134.

DANIEL, T. L. (1995). Invertebrate swimming: integrating internal and external mechanisms. In *Biological Fluid Dynamics* (ed. C. P. Ellington and T. J. Pedley), pp. 61–89. Cambridge: The Company of Biologists Ltd.

DE VAUGELAS, J. (1985). Sediment reworking by Callianassidae mud shrimp in tropical lagoons: a review with perspectives. *Proc. Fifth Int. Coral Reef Congr. Tahiti* **6**, 617–621.

DWORSCHAK, P. C. (1981). The pumping rates of the burrowing shrimp *Upogebia pusilla* (Petagna) (Decapoda: Thalassinidea). *J. exp. mar. Biol. Ecol.* **52**, 25–35.

FARLEY, R. D. AND CASE, J. F. (1968). Perception of external oxygen by the burrowing shrimp, *Callianassa californiensis* Dana and *C. affinis* Dana. *Biol. Bull. mar. biol. Lab., Woods Hole* **134**, 361–365.

FELDER, D. L. (1979). Respiratory adaptations of the estuarine mud shrimp, *Callianassa jamaicense* (Schmitt, 1935) (Crustacea: Thalassinidea). *Biol. Bull. mar. biol. Lab., Woods Hole* **152**, 134–146.

FORSTER, S. AND GRAF, G. (1995). Impact of irrigation on oxygen flux into the sediment: intermittent pumping by *Callianassa subterranea* and 'piston-pumping' by *Lanice conchilega*. *Mar. Biol*. **123**, 335–346.

GUST, G. AND HARRISON, J. T. (1981). Biological pumps at the sediment–water interface: Mechanistic evaluation of the Alpheid shrimp *Alpheus mackayi* and its irrigation pattern. *Mar. Biol*. **64**, 71–78.

HOERNER, S. F. (1965). *Fluid-dynamic Drag.* Bricktown, NJ: Hoerner Fluid Dynamics.

KOIKE, I. AND MUKAI, H. (1983). Oxygen and inorganic nitrogen conditions and their fluxes in the burrow of *Callianassa japonica* [de Haan] and *Upogebia major* [de Haan]. *Mar. Ecol. Progr. Ser.* **12**, 185–190.

MORRIS, M. J., GUST, G. AND TORRES, J. J. (1985). Propulsion efficiency and cost of transport for copepods: a hydromechanical model of crustacean swimming. *Mar. Biol.* **86**, 283–295.

MORRIS, M. J., KOHLHAGE, K. AND GUST, G. (1990). Mechanics and energetics of swimming in the small copepod *Acanthocyclops robustus* (Cyclopoida). *Mar. Biol.* **107**, 83–91.

MUKAI, H. AND KOIKE, L. (1984). Pumping rates of the mud shrimp *Callianassa japonica*. *J. Oceanogr. Soc. Japan* **40**, 243–246.

MUNSON, B. R., YOUNG, D. F. AND OKIISHI, T. H. (1994). *Fundamentals of Fluid Mechanics*.Second edition. New York: John Wiley & Sons.

PRANDTL, L. AND TIETJENS, O. G. (1957). *Applied Hydro- and Aeromechanics* (replica of 1934 edition). New York: Dover Publications.

ROWDEN, A. A. AND JONES, M. B. (1995). The burrow structure of the mud shrimp *Callianassa subterranea* (Decapoda: Thalassinidea) from the North Sea. *J. nat. Hist.* **29**, 1155–1165.

SCHLICHTING, H. (1979). *Boundary-Layer Theory*. Seventh edition. New York: McGraw-Hill.

SCOTT, P. J. B., REISWIG, H. M. AND MARCOTTE, B. M. (1988). Ecology, functional morphology, behaviour and feeding in coral- and sponge-boring species of *Upogebia* (Crustacea: Decapoda: Thalassinidea). *Can. J. Zool*. **68**, 483–495.

STAMHUIS, E. J., REEDE-DEKKER, T., ETTEN, Y., VAN WILJES, J. J. AND VIDELER, J. J. (1996). Behaviour and time allocation of the burrowing shrimp *Callianassa subterranea* (Decapoda, Thalassinidea). *J. exp. mar. Biol. Ecol*. **204**, 225–239.

STAMHUIS, E. J., SCHREURS, C. E. AND VIDELER, J. J. (1997). Burrow architecture and turbative activity of the thalassinid shrimp *Callianassa subterranea* from the central North Sea. *Mar. Ecol. Prog. Ser*. **151**, 155–163.

STAMHUIS, E. J. AND VIDELER, J. J. (1997*a*). Burrow ventilation in the tube-dwelling shrimp *Callianassa subterranea* (Decapoda: Thalassinidea). I. Morphology and motion of the pleopods, uropods and telson. *J. exp. Biol*. **201**, 2151–2158.

STAMHUIS, E. J. AND VIDELER, J. J. (1997*b*). Burrow ventilation in the tube-dwelling shrimp *Callianassa subterranea* (Decapoda: Thalassinidea). II. The flow in the vicinity of the shrimp and the energetic advantages of a laminar non-pulsating ventilation current. *J. exp. Biol*. **201**, 2159–2170.

TORRES, J. J., GLUCK, D. L. AND CHILDRESS, J. J. (1977). Activity and physiological significance of the pleopods in the respiration of *Callianassa californiensis* (Dana) (Crustacea: Thalassinidea). *Biol. Bull. mar. biol. Lab., Woods Hole* **152**, 134–146.

VOGEL, S. (1994). *Life in Moving Fluids: the Physical Biology of Flow*. Second edition. Princeton, NJ: Princeton University Press.

WITBAARD, R. AND DUINEVELD, G. C. A. (1989). Some aspects of the biology and ecology of the burrowing shrimp *Callianassa subterranea* (Montagu) (Thalassinidea) from the Southern North Sea. *Sarsia* **74**, 209–219.